14th International Beam Instrumentation Conference,Liverpool, UK JACoW Publishing
ISBN: 978-3-95450-262-2 ISSN: 2673-5350 doi: 10.18429/JACoW-IBIC2025-TUPCO15

FAST CORRECTOR VESSEL SELECTION FOR HIGH BANDWIDTH FAST ORBIT FEEDBACK

S. Banerjee*, F. Malinowski, L. Bobb, Diamond Light Source, Didcot, United Kingdom

Abstract

The DiamonDiamond-II upgrade will enhance the performance of the Diamond Light Source synchrotron, including improved beam stability by the Fast Orbit Feedback system. Achieving the targeted closed-loop bandwidth of 1 kHz necessitates an open-loop actuator bandwidth of approximately 10 kHz, which presents significant design challenges for the corrector magnet vacuum vessel. Additionally, subsystems such as the corrector magnet power supplies and Beam Position Monitors must comply with a stringent closed-loop latency of less than 100 µs. Initially, a 1 mm stainless steel vessel was deemed viable; however, experimental findings indicated that the combination of stainless steel and neighbouring copper vessels resulted in a decrease in both integrated magnetic field strength and system bandwidth. This prompted a reassessment of the material selection for the fast corrector vessels to optimise orbit feedback performance. This paper investigates these challenges, analyses experimental data, and explores solutions to achieve the necessary bandwidth for the DiamonDiamond-II upgrade.

INTRODUCTION

The Diamond-II upgrade project significantly enhances Diamond Light Source (DLS) synchrotron performance through a Fast Orbit Feedback (FOFB) system targeting 1 kHz closed-loop bandwidth. The FOFB controller manages 252 slow correctors (SCs) and 138 fast correctors (FCs) using generalised singular value decomposition (GSVD)-based dual-rate Internal Model Control (IMC) for efficient handling of two-input-single-output (TISO) and single-input-single-output (SISO) subsystems [1].

The system architecture requires 10 kHz open-loop bandwidth for FCs and 150 Hz for SCs [1], creating substantial challenges for FC magnet vacuum vessel material selection. Additionally, the FOFB subsystem requirements include FC magnet power supply units (PSUs) and Beam Position Monitors (BPMs) with Analogue Front-End (AFE), Digital Signal Processing (DSP) filters, and Digital-to-Analogue Converters (DACs) meeting <100 µs closed-loop latency specifications [1–3].

Initial analysis using the Podobedov model [4] indicated 1 mm thick stainless steel (SS) vessels could theoretically achieve the required bandwidth. However, experimental findings revealed unexpected complications when combining SS vessels with neighbouring copper (Cu) vessels, reducing integrated magnetic field strength and overall open-loop bandwidth [5]. This discovery necessitated material selection re-evaluation for Diamond-II FOFB FC vessels.

* shohan.banerjee@diamond.ac.uk

Given the permanent vessel installation and impracticality of post-installation replacement, optimal material selection is critical for the success of Diamond-II. This paper explores vessel material selection challenges, analyses experimental results, and proposes solutions to achieve desired bandwidth performance.

VESSEL TRANSFER FUNCTION

To evaluate the transfer function (TF) of FC vessels, several assumptions were made:

- All vessels will have a length of 85 mm with a thickness of 1 mm, combined with neighbouring Cu vessels.
- The magnetic field is symmetric across the vessel on both sides of the FC magnet.
- The behaviour in the vertical and horizontal directions is identical.

These assumptions provide a consistent basis for comparing different vessel materials and their effects on the FOFB system performance.

Experimental Data

The Magnet Group at DLS carried out experimental studies using a prototype FC magnet with three 85 mm-long and 1 mm thick vessels. The three configurations were stainless steel (SS) joined to Cu, Inconel joined to Cu, and titanium (Ti) joined to Cu, as shown in Fig. 1(a). For consistency, the Cu sections were manufactured to the same diameter and thickness as the SS vessel. The vessel components were friction-fitted rather than permanently joined; this had only a minor effect on the measured bandwidths, which also showed good agreement with OPERA 3D simulations.

A sinusoidal signal from 10 Hz to 30 kHz was generated and applied to a narrow, long multi-turn search coil as shown in Fig. 1(b), placed at the geometric centre of the vessel shown in Fig. 1(c). All measurements were done using a Zurich Instruments MFLI lock-in amplifier. Its output drove the magnet coil, creating an oscillating magnetic field. A search coil detected the induced voltage, which was fed back into the lock-in input. By sweeping the frequency, repeatable measurements were achieved with minimal noise.

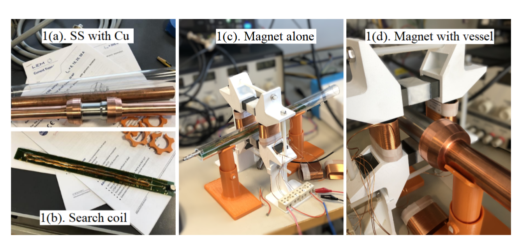

Figure 1: Experimental setup of prototype FC.

ISBN: 978-3-95450-262-2 ISSN: 2673-5350 doi: 10.18429/JACoW-IBIC2025-TUPCO15

Measurements were taken for the magnet alone (baseline) as shown in Fig. 1(b) and for the magnet combined with each vessel as shown in Fig. 1(d). The transfer function (amplitude and phase) was obtained by dividing the magnet with vessel response by the magnet-only response. This experiment provided valuable data on the frequency response of different vessel materials and their transfer functions.

System Identification

Based on the experimental data, a system identification was performed to evaluate the TF using MATLAB [6]. The following steps were taken to evaluate the transfer function:

- Due to noise in the low-frequency data, several indices were eliminated from this region and replaced with zero. Data smoothing was also applied to reduce measurement noise.
- The magnitude scale was converted from logarithmic to linear, and the frequency scale was converted from 'Hz' to 'rad/s.'
- Frequency responses for both SS, Inconel, and Ti were created using the magnitude and phase data.
- An identified frequency domain data model was generated using the $idfrd$ command.
- It was assumed that the transfer functions would have two poles and one zero, as this configuration produced the best estimations.
- Finally, the $tfest$ command was used to evaluate the transfer functions.

It is important to note that the TF for vertical and horizontal planes is identical, due to the symmetric geometry and material properties of the vessel.

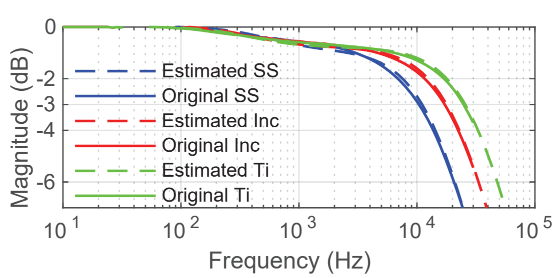

Figure 2: Experimental data and estimated transfer function for the 85 mm SS, Inconel, and Ti vessel.

Figure 2 compares the transfer functions estimated using MATLAB system identification with experimental data for the different vessels. The results indicate that the frequency-domain performance (up to 3 kHz) of the SS, Inconel, and Ti vessels is nearly identical. At higher frequencies (>3 kHz), however, the Inconel and Ti vessels show slightly improved performance. A minor rollover of approximately −0.85 dB is observed in the 200 Hz to 700 Hz range, preceding the main rollover at around 10 kHz. This intermediate is attributed to electromagnetic coupling effects resulting from the combination of SS/Inconel/Ti vessel with neighbouring Cu vessels configurations.

The estimated transfer functions for different vessels are represented by Eq.(1)-(3).

$$TF_{\mathrm{SS}}(s) = \frac{7.953E4s + 2.903E8}{s^2 + 9.123E4s + 2.895E8}, \tag{1}$$

$$TF_{\mathrm{Inc}}(s) = \frac{1.253E5s + 3.267E8}{s^2 + 1.394E5s + 3.242E8}, \tag{2}$$

$$TF_{\mathrm{Ti}}(s) = \frac{1.804E5s + 4.563E8}{s^2 + 1.997E4s + 4.554E8}, \tag{3}$$

where $s \in \mathbb{C}$ is the Laplace variable and TF_{SS}, TF_{Inc}, and TF_{Ti} represent the corresponding transfer functions for the 85 mm SS vessel, Inconel vessel, and Ti vessel, respectively.

COMPOSITE TRANSFER FUNCTION

The frequency responses from all other components PSU, DSP filter, DAC, and AFE were considered to estimate the composite TF. A frequency response was constructed for all vessel types. This frequency domain signal was then used for the composite TF estimation in MATLAB's built-in identification application [6]. To determine the composite TF a third-order system with a zero in the left half of the $s-plane$ provided the best fit for the composite TF as shown in Fig. 3. However, the roll-off above 10 kHz of the original response was slightly faster than the estimated one. As this frequency range is beyond the current scope of interest, it was disregarded.

It is important to note that, during the TF estimation process, the delay was initially removed from both the parent and estimated signals. After determining the TF, a delay of 100 µs was reintroduced to both signals. The estimated composite transfer functions with delay for SS, Inconel, and Ti are given in Eqs. (4)-(6), respectively. The resulting bandwidth comparison with the corresponding data presented in Table 1.

$$TF^{C}_{\mathrm{SS}}(s) = \frac{3.26E10s + 9.85E13}{s^3 + 6.621E5s^2 + 3.894E10s + 9.88E13}e^{-\tau s}, \tag{4}$$

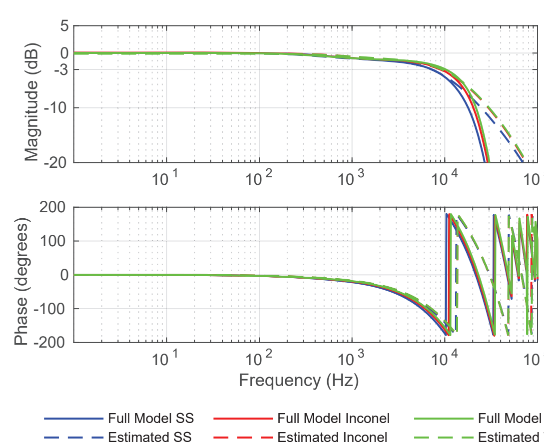

Figure 3: Frequency response of composite TF of FC with different vessels.

ISBN: 978-3-95450-262-2 ISSN: 2673-5350 doi: 10.18429/JACoW-IBIC2025-TUPCO15

$$TF^{C}_{\text{Inc}}(s) = \frac{3.16E10s + 1.95E14}{s^3 + 5.441E5s^2 + 3.894E10s + 1.96E14} e^{-\tau s}, \tag{5}$$

$$TF^{C}_{\text{Ti}}(s) = \frac{3.28E10s + 1.97E10^{14}}{s^3 + 5.552E5s^2 + 3.984E10s + 1.997E14} e^{-\tau s}, \tag{6}$$

where $s \in \mathbb{C}$ is the Laplace variable, τ is the total time delay of the FC 100 µs, and TF^C_{SS}, TF^C_{Inc}, and TF^C_{Ti} represent the corresponding composite transfer functions for the 85 mm SS, Inconel, and Ti vessels, respectively.

Table 1: Estimated Bandwidth of Transfer Functions for Different 85 mm Long Vessel Materials

Vessel Type	Vessel + Magnet TF (Hz)		Composite TF (Hz)	
	X	Y	X	Y
SS	10722	10722	7375	7375
Inconel	17073	17073	9331	9331
Ti	24770	24770	10022	10022

SIMULATION RESULTS

The electron beam dynamics at Diamond-II can be expressed as

$$\mathbf{y}(s) = \mathbf{R}_s g_s(s)\mathbf{u}_s(s) + \mathbf{R}_f g_f(s)\mathbf{u}_f(s) + \mathbf{d}(s), \tag{7}$$

where s is the Laplace variable, and the subscripts s and f denote SC and FC respectively. Here, $\mathbf{y}(s)$, $\mathbf{u}_s(s)$, $\mathbf{u}_f(s)$, and $\mathbf{d}(s)$ represent the beam position, SC input, FC input, and disturbances, respectively. The matrices $\mathbf{R}_s$ and $\mathbf{R}_f$ are the orbit response matrices (ORMs) for the SC and FC, while $g_s(s)$ and $g_f(s)$ are their respective scalar transfer functions. Equation (7) indicates that to maintain the same beam dynamics, a reduction in FC bandwidth $g_f(s)$ requires a corresponding increase in FC input demand.

The composite TF of the FC was used to simulate the FOFB model with a regularisation parameter of $\mu = 0.01$ [7]. The overall beam dynamics remained consistent across all vessel types (SS, Inconel, and Ti). Figure 4 shows the horizontal Integrated Beam Motion (IBM) at primary BPMs on long-straight (LS) sections for SS, Inconel, and Ti vessels. Similar behaviour was observed at other BPMs (e.g., mid-straight (MS) and short-straight (SS), in both planes), but those results are omitted for brevity.

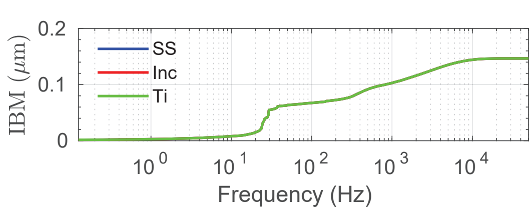

Figure 4: IBM plots with three different vessels in LS.

While the IBM patterns are identical across vessel types, the power demands differ as shown in Table 2. The SS vessel, with the lowest bandwidth, requires the highest PSU power, while the Ti vessel, with the highest bandwidth, requires the least. Thus, although bandwidth variations do not significantly affect beam dynamics, they strongly influence PSU current and voltage demands.

Table 2: Fast Corrector Power Demand for 85 mm Vessels

Quantity	Vessel Type	Maximum Demand	
		X	Y
Current (mA)	SS	< 166.6	< 91.6
	Inconel	< 162.3	< 87.8
	Ti	< 161.1	< 86.9
Voltage (V)	SS	< 5.6	< 3.6
	Inconel	< 5.0	< 3.2
	Ti	< 4.9	< 3.2

Overall, simulations confirm that all vessel types are suitable for FC applications. The composite TF aligns better with the higher bandwidth of Inconel and Ti vessels, which also reduces PSU power requirements. However, the performance of the composite TF, hence the FC magnet demand, may vary if the TF of PSU or other influencing factors change, potentially altering the current and voltage requirements. For Diamond-II disturbances, due to uncertainties, a worst-case scenario was assumed based on Ref. [7]. FC magnet demand may therefore vary depending on the actual disturbance profile. Since the FC magnet demand is a critical factor in vessel selection, it must be carefully evaluated alongside dynamic performance.

CONCLUSION

It is evident from the analysis that whichever vessel material is selected for the FC, it will inevitably be influenced by the neighbouring Cu vessels. This effect cannot be eliminated and must be taken into account. If the FC vessel length is approximately 85 mm, any of the tested materials (SS, Inconel, or Ti) can be employed. Inconel and Ti are marginally preferable due to their slightly higher bandwidth.

Cost is also an important factor in material selection. While SS is the least expensive and Ti the most costly, Ti offers little advantage over Inconel in terms of magnet demand performance. Given the performance–cost balance, Inconel is the most practical choice for Diamond-II FCs.

In practice, certain geometric constraints in Diamond-II prevent achieving the full 85 mm FC length at some locations. A shorter vessel length further reduces the available bandwidth. In such cases, Ti becomes the preferable option because of its higher intrinsic bandwidth helps reduce the overall power demand despite the reduced length.

ACKNOWLEDGEMENTS

The authors express their gratitude to Arash Amiri and the Power Supply group at DLS for providing the TF of FC.

ISBN: 978-3-95450-262-2 ISSN: 2673-5350 doi: 10.18429/JACoW-IBIC2025-TUPCO15

REFERENCES

[1] I. Kempf, M. G. Abbott, L. Bobb, G. B. Christian, S. Duncan, and G. Rehm, "Fast Orbit Feedback for Diamond-II", in *Proc. IBIC'23*, Saskatoon, Canada, Sep. 2023, pp. 1–6. doi:10.18429/JACoW-IBIC2023-MO2I02

[2] I. Kempf, G. B. Christian, M. Abbott, L. Bobb, P. J. Goulart, and S. R. Duncan, "Control of Multi-Array Cross-Directional Systems Using the Generalised Singular Value Decomposition", *Automatica*, vol. 179, p. 112431, 2025. doi:10.1016/j.automatica.2025.112431

[3] M. G. Abbott *et al.*, *Diamond-II Technical Design Report*, Diamond Light Source, Oxfordshire, UK, Tech. Rep., Aug. 2022. https://www.diamond.ac.uk/Home/News/LatestNews/2022/14-10-22.html

[4] B. Podobedov, H. Witte, and M. Blaskiewicz, "Eddy Current Shielding of the Magnetic Field Ripple in the EIC Electron Storage Ring Vacuum Chambers", in *Proc. IPAC'24*, Nashville, TN, USA, 2024, paper MOPC77. doi:10.18429/JACoW-IPAC2024-MOPC77

[5] S. H. Mirza *et al.*, "PETRA IV: New Dimensions – Progress and Challenges of FOFB System", presented at the 10th Diagnostics Experts of European Light Sources (DEELS) Workshop, DESY, Hamburg, Germany, Jun. 19–21, 2023, unpublished.

[6] System Identification using MATLAB, https://www.mathworks.com/help/releases/R2022a/pdf_doc/ident/ident_ref.pdf

[7] S. Banerjee, M. G. Abbott, L. Bobb, and I. Kempf,"Modified Fast Orbit Feedback Controller for Disturbance Attenuation in Long Straights for Diamond-II", in *Proc. IBIC'23*, Saskatoon, Canada, Sep. 2023, pp. 119–122. doi:10.18429/JACoW-IBIC2023-MOP041